

# Performance characteristics of a proton-transfer-reaction mass spectrometer (PTR-MS) derived from laboratory and field measurements

M. Steinbacher<sup>a,1</sup>, J. Dommen<sup>a,\*</sup>, C. Ammann<sup>b</sup>, C. Spirig<sup>b</sup>, A. Neftel<sup>b</sup>, A.S.H. Prevot<sup>a</sup>

<sup>a</sup> *Laboratory of Atmospheric Chemistry, Paul Scherrer Institut, CH-5232 Villigen PSI, Switzerland*

<sup>b</sup> *Agroscope FAL, Air Pollution/Climate Group, P.O. Box, CH-8046 Zurich, Switzerland*

Received 25 July 2003; accepted 7 July 2004

Available online 25 September 2004

## Abstract

Volatile organic compounds (VOCs) play an important role in the formation of ozone and aerosols in the atmosphere. In an increasing number of field campaigns the proton-transfer-reaction mass spectrometer (PTR-MS) has proven to be a useful and fast tool for measuring VOCs and studying the relevant atmospheric processes. This work describes laboratory and field measurements with two different versions of the PTR-MS and presents important instrument specific features. The temperature stabilization and the change of the gasket material in the newer version significantly improved the performance of the instrument, as demonstrated by periodical background measurements under field conditions. The investigation of the mass discrimination illustrated the necessity of an elaborate verification. The humidity dependence of benzene was substantially lower than in former studies, which used higher drift tube pressures, but it is still higher than predicted by a simple dimer/monomer equilibrium model. An instrument comparison with a fluorescent technique was performed for formaldehyde and showed differences between pure formaldehyde calibration gases and complex ambient air samples. An intercomparison of two PTR-MSs measuring ambient air yielded satisfactory results after calibration for most of the considered masses. Comparing PTR-MS and gas chromatograph measurements of aromatic compounds, revealed a good agreement for conditions of fresh anthropogenic emissions. In photochemically aged air, many masses detected by the PTR-MS are not only influenced by anthropogenically and biogenically emitted but also oxidized VOCs.

© 2004 Elsevier B.V. All rights reserved.

**Keywords:** Proton-transfer-reaction mass spectrometry; Volatile organic compounds; Humidity dependence; HCHO comparison

## 1. Introduction

The proton-transfer-reaction mass spectrometer (PTR-MS) was developed by Lindinger and co-workers at the University of Innsbruck, Austria [1]. A multitude of PTR-MS related publications have appeared in environmental sciences (e.g., [2–4]), food analysis (e.g., [5–7]) and medical applications (e.g., [8–11]) within the last years.

Early publications about the PTR-MS claimed that it is not necessary to perform regular calibrations for different

volatile organic compounds (VOCs) [1,12–14] as long as instrument-specific parameters (like the transmission function and the residence time of the primary ions in the reaction chamber) as well as the compound-dependent reaction rate constants for the protonation of these VOCs are known. The rate constants can theoretically be calculated with the aid of empirical relations [15–17]. Hansel et al. [14] estimated the accuracy of the VOC mixing ratio measurements to 30%, mainly caused by the uncertainties of the reaction rate constants, which are up to  $\pm 20\%$ . Other instrument- and configuration-specific experimental effects were not considered relevant. Recent publications postulate a detailed characterization and calibration of the PTR-MS by means of gas standards [18–20]. However, as the instrument can measure a large amount of different substances and gas standards are

\* Corresponding author. Tel.: +41 56 310 2992; fax: +41 56 310 4525.

E-mail address: [josef.dommen@psi.ch](mailto:josef.dommen@psi.ch) (J. Dommen).

<sup>1</sup> Present address: Swiss Federal Laboratories for Materials Testing and Research (EMPA), Air Pollution/Environmental Technology Laboratory, CH-8600 Duebendorf, Switzerland.

not available for all compounds, the concentrations of various compounds still need to be calculated from the count rates according to the theory. Therefore, the assumptions used for the calculation of concentrations need to be checked carefully.

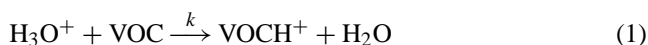
This paper presents important characterizations of the instrument concerning the temperature dependence of the background signal, the humidity dependence of the sensitivity and the determination of the transmission function. Furthermore, comparison measurements of ambient concentrations of the PTR-MS with a gas chromatograph and a formaldehyde monitor are shown.

## 2. Experimental

### 2.1. PTR-MS methodology

The PTR-MS instrument (IONICON Analytik GmbH, Innsbruck, Austria) has been described in detail in numerous publications elsewhere [1,12–14,21,22]. Therefore, just a short description is given here. The measuring method is based on a proton-transfer reaction of hydronium ions ( $\text{H}_3\text{O}^+$ ) to compounds with a higher proton affinity than water and subsequent detection of the product ions in a quadrupole mass spectrometer. For investigations of trace components in air,  $\text{H}_3\text{O}^+$  is a suitable proton donor because the primary ions do not react with any of the common constituents in air like nitrogen, oxygen, carbon dioxide, carbon monoxide, methane, and ozone. Most common VOCs in the atmosphere, excluding the alkanes and small alkenes/alkynes exhibit sufficient proton affinities [23]. The proton-transfer ionization takes place at relatively low energies, and therefore, causes only little fragmentation of most of the ion products. However, it can have a considerable effect for some specific compounds like isoprene [24] and the monoterpenes [25].

A hollow cathode discharge generates  $\text{H}_3\text{O}^+$  and a number of other ions ( $\text{H}^+$ ,  $\text{O}^+$ ,  $\text{H}_2^+$ ,  $\text{OH}^+$ ,  $\text{H}_2\text{O}^+$ ) from pure water vapor. Afterwards the ions pass a source drift region where ions other than  $\text{H}_3\text{O}^+$  are almost completely converted to  $\text{H}_3\text{O}^+$ . Subsequently, the  $\text{H}_3\text{O}^+$  ions enter the drift tube, that is continuously flushed with the sample air at a pressure of slightly higher than 2 mbar. In the drift tube VOCs are ionized according to the following reaction:



If the VOCs are present in quantities below a few parts per million, the  $\text{H}_3\text{O}^+$  ions do not decrease significantly such that  $[\text{VOC}] \gg [\text{H}_3\text{O}^+] \gg [\text{VOCH}^+]$  is valid. The number density of a VOC in the lower ppb range adds up to around  $10^8$  molecules  $\text{cm}^{-3}$  at typical drift tube conditions, the  $\text{H}_3\text{O}^+$  concentration in the drift tube is approximately  $10^4$  ions  $\text{cm}^{-3}$  (A. Hansel, personal communication). The residence time of the air to be analyzed is around 0.1 s. This results in a VOC

decrease due to Eq. (1) of 0.0002% taking into account typical primary ion concentrations and reaction rate constants. Assuming a total VOC loading of 1 ppm and considering a residence time of the ions in the drift tube of around 100  $\mu\text{s}$ , the proton-transfer reaction leads to a  $\text{H}_3\text{O}^+$  ions decay of around 1%.

In brief, due to the short reaction time neither the VOCs nor the primary ions decrease significantly due to reaction (1). Under these conditions, and taking into account the mass-dependent transmission of the instrument, the number density of a certain compound can be calculated from the following equation:

$$[\text{VOC}] = \frac{[\text{VOCH}^+] \text{trans}(\text{H}_3\text{O}^+)}{[\text{H}_3\text{O}^+] \text{trans}(\text{VOCH}^+) kt} \quad (2)$$

where  $t$  is the residence time of the primary ions in the drift tube (typically circa 100  $\mu\text{s}$ ),  $k$  is the proton-transfer reaction rate constant which corresponds to the ion-molecule capture collisions and  $\text{trans}(\dots)$  is the mass dependent transmission for the respective ions.  $[\text{VOCH}^+]$  and  $[\text{H}_3\text{O}^+]$  are taken from the ion signals of the protonated VOC and the primary ion, respectively. Typical count rates of the primary ions are 4–5 Mio cps (counts per second). Therefore, it is feasible to measure the  $^{18}\text{O}$  isotope of the primary ion ( $\text{H}_3^{18}\text{O}^+$ ;  $m/z$  21) to avoid reaching the saturation range and to reduce aging effects of the detector. Due to an isotope ratio  $^{18}\text{O}/^{16}\text{O}$  of 0.20% [26], the  $m/z$  21-signal has to be multiplied by 500 to obtain the primary ion counts. The reaction rate constants can be calculated based on different theories [16,17,27,28], they include an uncertainty of  $\pm 20\%$  [12,14]. In the following, the Langevin theory [27] was used for molecules with an unknown or without dipole moment. For molecules with a permanent dipole moment, the reaction rates were determined according to the parameterizations based on trajectory calculations done by Chesnavich et al. [28] and Su and Chesnavich [17].

A secondary electron multiplier detects the primary and the product ions after passing a quadrupole mass spectrometer. The electron multiplier is attached perpendicular to the hollow cathode, the drift tube, and the quadrupole mass spectrometer to minimize the background signal. Photons and fast neutral particles can also trigger a pulse at the electron multiplier. This effect can be suppressed by this perpendicular configuration. An electrostatic field deflects the ions between the quadrupole and the detector. As the deflection is mass-dependent, it influences the transmission in Eq. (2). The transmission is also reduced due to ion losses between the drift tube and the quadrupole.

Another approach to derive VOC mixing ratios is based on calibrating the instrument with gas standards and calculating the concentrations by using appropriate calibration factors. But, as the instrument can measure a large amount of different substances and gas standards are not available for all compounds, the determination of the concentrations with Eq. (2) is still needed.

## 2.2. PTR-MS set-up

Performance tests and measurements of two instruments are presented in this work. The first has been operated by Agroscope FAL (Federal Research Station for Agroecology and Agriculture), since 2000 and is referred to as the PTR-MS (FAL). The second is a newer version of the instrument, operated by the Paul Scherrer Institut since 2002, denoted as PTR-MS (PSI) hereafter. The PTR-MS (FAL) had a drift tube of 9.5 cm length and 5 cm diameter and was equipped with Viton gaskets. Until September 2001, ambient air was aspirated through a mass flow controller and perfluoroalkoxy (PFA) tubings before entering the drift tube. The mass flow controller was then replaced by a pressure flow controller in a bypass, as it is now standard for this instrument. The newer instrument, the PTR-MS (PSI), is optimised concerning a faster response, temperature stabilization, and gasket and tubing materials. It is equipped with a drift tube of 9.25 cm length and of 1.4 cm diameter and teflon gaskets. The inlet tubes are made out of Silcosteel<sup>®</sup>. The inlet system and the drift tube of this instrument are kept at a constant temperature of 50 °C to reduce the temperature dependent variations of the background signal. The blank values were measured passing the ambient air through a Supelpure<sup>™</sup> charcoal cartridge (Supelco, Bellefonte PA, USA).

## 2.3. Other VOC analyzers

Both mass spectrometers were operated in the laboratory as well as in the field in parallel to other state of the art methods for VOC measurements like gas chromatography for hydrocarbons and a fluorescent technique for formaldehyde.

A commercial Airmotec HC1010 gas chromatograph (ChromatoSud, Saint Antoine, France) was used to measure hydrocarbons between C<sub>4</sub> (hydrocarbons containing four carbon atoms) and C<sub>10</sub> [29]. Sample air is pulled through adsorption tubes containing Carbopack B and Carbosieve III. After desorbing, the hydrocarbons are cryofocused, using a fused silica capillary packed with Carbopack B and cooled with CO<sub>2</sub>. Injection onto the chromatographic column proceeds after fast desorption at 350 °C. The stationary phase of the separation column consists of 2.5% phenyl and 97.5% methylpolysiloxan (BGB Analytik AG, Anwil, Switzerland). A flame ionisation detector (FID) is used for detection. The instrument was operated in a mode to obtain concentrations averaged over 30 min.

Formaldehyde (HCHO) was continuously measured with the Hantzsch method as described by Kelly and Fortune [30]. HCHO is collected in a glass coil scrubber. The scrubbing solution is mixed with the Hantzsch solution (mixture of acetic acid, acetylacetone and ammonium acetate). A fluorescent derivative is formed from a reaction of formaldehyde with ammonium acetate and acetylacetone in a heated reaction coil. The produced diacetyldihydrolutidine (DDL) is then detected by fluorimetry. The excitation and emission wavelengths are 400 and 510 nm, respectively.

## 2.4. Measurement locations

A field campaign including a comparison of PTR-MS (FAL) and gas chromatograph (Airmotec HC1010) measurements took place in Berne, Switzerland in March 2001. Ambient air was measured on the top of a 15 m high building close to a road with heavy traffic. The intention of the campaign was an assessment of urban ammonia emissions and their correlation to VOC emissions.

In August and September 2001, the PTR-MS (FAL) was operated in parallel to the formaldehyde monitor for measurements of ambient air within the scope of the CHAPOP (Characterization of High Alpine Pollution Plumes) campaign in the Leventina valley, southern Switzerland. The measurements were performed in a rural environment at 1240 m above sea level and about 500 m above the valley ground, where one of the major trans-alpine traffic routes passes by. The aim was to enhance the knowledge of photochemical processes and vertical transport of air pollutants in the high Alpine atmosphere.

Further measurements were performed in the Po Basin in Northern Italy in summer 2002 in the framework of the EU project FORMAT (Formaldehyde as a Tracer of Photooxidation in the Troposphere) project. The instruments were located in a semi-rural environment, which was sometimes influenced by the plume of Milan. These measurements will be used to investigate the formaldehyde formation processes and the role of formaldehyde in photochemistry.

## 3. Results and discussion

### 3.1. Temperature dependence of the background signal

During the CHAPOP campaign, the PTR-MS (FAL) was located in an air-conditioned trailer. Because of problems with the air conditioning, a significant diurnal variation of the temperature with a daily amplitude up to 14 °C occurred inside the container during some sunny days. The blank values were measured every 3 h for 30 min. The diurnal patterns of the indoor temperature and the blank values of benzene (*m/z* 79), C<sub>2</sub>-benzenes (*m/z* 107) and C<sub>3</sub>-benzenes (*m/z* 121) are shown in Fig. 1. The PTR-MS mass signals were converted to mixing ratios according to Eq. (2).

The blank values of all three masses strongly depended on the indoor temperature. Laboratory tests showed that this effect could not be related to a changing efficiency of the charcoal cartridge within the observed temperature range.

The observed temperature and pressure variation from 16 to 30 °C and from 2.03 to 2.09 mbar affect the residence time of the primary ions in the drift tube by about 2%. The calculated reaction rate constants change only marginally. Therefore, the temperature and pressure dependence of the residence time and the reaction rate constants for the protonation cannot explain the variability.

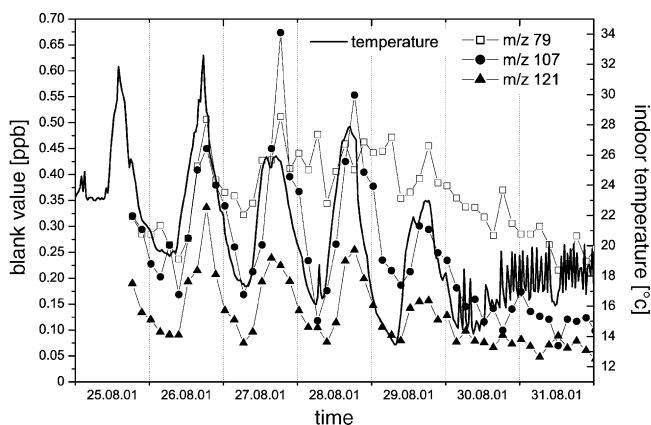


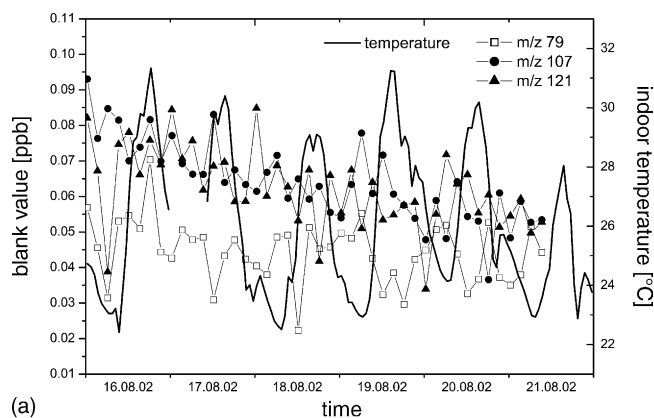
Fig. 1. Indoor temperature and calculated blank value mixing ratios according to Eq. (2) of benzene ( $m/z$  79),  $C_2$ -benzenes ( $m/z$  107) and  $C_3$ -benzenes ( $m/z$  121) for a 7-day-period during the CHAPOP field campaign in southern Switzerland.

During the FORMAT campaign, similar problems with the temperature control in the measurement container occurred and the instrument was exposed to diurnal temperature variations of up to 8 °C. These measurements were performed with the temperature stabilized PTR-MS (PSI). No correlation between the indoor temperature and the background could be observed this time (Fig. 2a).

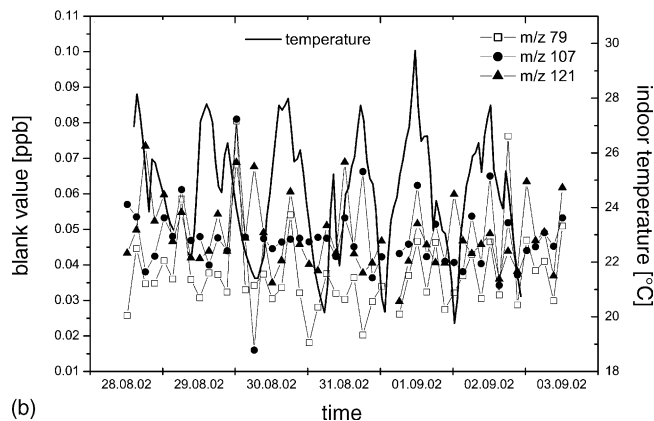
The slight decrease of the background signal for  $m/z$  107 and 121 during the first 6-day-period is most probably related to the new secondary electron multiplier (SEM) that was installed at 12 August, 2002. A new SEM can exhibit an increased background signal for approximately 1 week (A. Jordan, IONICON, personal communication) and should then fade continuously. This is corroborated by data acquired 2 weeks after installation of the SEM in Fig. 2b. The background has not decreased significantly anymore and has reached a constant level.

Besides a much lower variability, the absolute background values of the PSI-instrument are much lower, too. The average blank values (and the standard deviations) of the FAL-instrument for the period shown in Fig. 1 are 0.36 ppb (0.08 ppb) for  $m/z$  79, 0.25 ppb (0.13 ppb) for  $m/z$  107, and 0.13 ppb (0.06 ppb) for  $m/z$  121, respectively. For comparison, the blank values of the PSI-instrument during the period, shown in Fig. 2b, amount to 0.04 ppb (0.01 ppb) for  $m/z$  79, and 0.05 ppb (0.01 ppb) for  $m/z$  107 and 121.

The background variability is most likely related to impurities in the instrument that are desorbed more efficiently at higher temperatures. It explains the lower variations of the PSI instrument with its temperature controlled drift tube. Besides the temperature stabilization, the change of the gasket material from Viton to Teflon might also have improved the system. GC-PTR-MS measurements performed by Warneke et al. [31] showed broad peaks when using Viton gaskets and sharper peaks when using Teflon. They are attributing this phenomenon to memory effects (adsorption and desorption processes) on the Viton.



(a)



(b)

Fig. 2. Indoor temperature and calculated blank value mixing ratios according to Eq. (2) of benzene ( $m/z$  79),  $C_2$ -benzenes ( $m/z$  107) and  $C_3$ -benzenes ( $m/z$  121) during the FORMAT field campaign in northern Italy: (a) for a 6-day-period 2 days after changing the secondary electron multiplier; (b) for a 7-day-period approximately 2 weeks after changing the SEM.

### 3.2. Mass discrimination

The detection efficiency of the instrument is mass dependent. The mass discrimination of the instrument is influenced by three factors: losses of ions between the drift tube and the quadrupole, mass characteristics of the quadrupole and the deflection between the quadrupole and the SEM. To calculate the mixing ratios, the (mass dependent) efficiency of the detection must be considered. A default curve for the mass discrimination is provided by the manufacturer. A new measurement of the transmission was performed in the following way.

The determination of the transmission for mass  $x$  is based on the comparison of the decline of the primary ions ( $m/z$  19 or the protonated water isotope,  $m/z$  21 ( $H_3^{18}O^+$ )) and the increase of the signal of mass  $x$ . To obtain observable signals, an air sample with a high concentration of a species with protonated mass  $x$  has to be fed to the instrument. Based on the characteristics of the instrument, the transmission for a mass between 100 and 110 is usually set equal 1 and the whole transmission curve can be determined relative to this reference by this technique. The transmission can be derived

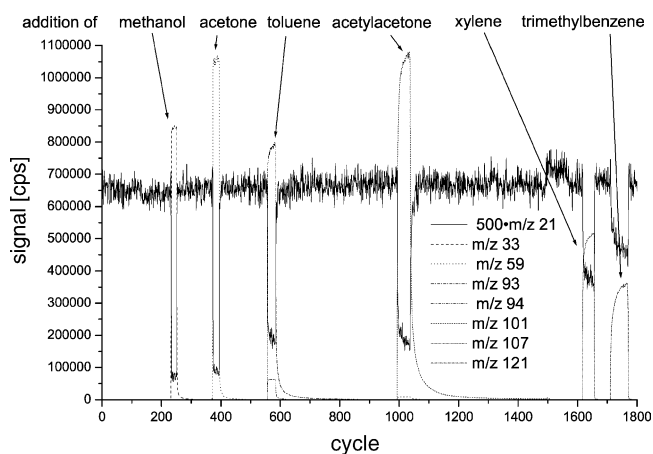


Fig. 3. Raw data for determination of the transmission of  $m/z$  33 (methanol),  $m/z$  59 (acetone),  $m/z$  93 (toluene),  $m/z$  101 (acetyl acetone),  $m/z$  107 (xylene), and  $m/z$  121 (trimethylbenzene).  $m/z$  94 ( $^{13}\text{C}$ -toluene) is added for illustration of the apparent  $^{13}\text{C}$ -isotopes. One cycle took 5 s.

by comparing the decline of the primary ions and the simultaneous increase of the mass  $x$  signal. Before starting the determination of mass discrimination, the primary ion signal was reduced from approximately 4 Mio cps to around 700,000 cps to avoid reaching the saturation of the SEM. Fig. 3 shows the raw data of a transmission curve determination experiment.

The measurements were performed with Tedlar gas sampling bags (1–4 l volume, Varian Inc., Palo Alto, CA, USA) filled with selected VOCs at ppm levels. These concentrations were obtained by injection of pure liquid solutions (Fluka Chemie GmbH, Buchs, Switzerland and Merck, Darmstadt, Germany, GC quality  $\geq 99.5\%$ ). After injecting the compound, the bags were filled with dry synthetic air. Around  $1\ \mu\text{l}$  of the pure compound per liter pillow bag volume was injected to yield an appropriate concentration. As the signal of the primary ions is increasing slightly with increasing humidity (as shown later, see Fig. 6), dry synthetic air was measured between switching the bags. Full scans were conducted to control if potential fragments or dimers could influence the mass discrimination measurements before the experiments. Only species without any significant fragmentation or dimer formation in the drift tube were used.  $^{13}\text{C}$ -isotopes were considered for the mass discrimination determination.

The results of several transmission measurements are summarized in Fig. 4. It is obvious that the experimentally determined curve significantly deviates from the (also experimentally determined) curve given by the manufacturer. Even when the two largest outliers are ignored, the discrepancy between the two different curves can amount up to 25%. The reason for this discrepancy may be attributed to different settings during the measurements, long-term drifts, or can be caused by the inaccuracy of a single transmission curve measurement. The error bars indicate the large scatter between the different measurements. Quadrupole mass spectrometers often have lower sensitivities for heavier ions because heavier ions spend more time in the fringing fields resulting in a larger

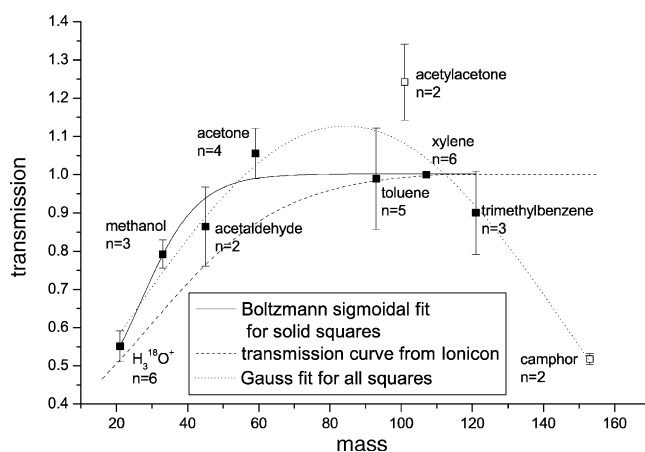


Fig. 4. Averaged transmission curve of the PTR-MS (PSI-instrument). The transmission for xylene (protonated mass, 107) was set equal 1. The error bars show the standard deviation. Number  $n$  specifies the number of measurements.

dispersion of the ions [32]. Therefore, the low transmission value for mass 153 (protonated camphor) might be explained by the fringing fields. As the use of the other compounds with similar masses failed due to significant fragmentation, it cannot be determined if it is a general characteristic of the PTR-MS or a camphor-specific effect. Full mass scans did not show any significant fragmentation of camphor in agreement with results published by Tani et al. [25]. Therefore, a possible fragmentation of camphor can be excluded as a source of error.

Recurring calibrations of the instrument with gas standards over around 10 months also show a variability of nearly  $\pm 30\%$ . If the scatter of the transmission is not related to the method of the determination itself, most of the variability of the calibration could be explained by the changing transmission properties of the PTR-MS. Surprisingly, the transmission curve of the PTR-MS (FAL) shows a smaller scatter [24], although the mass discrimination for both instrument was determined simultaneously with the same bags and the same concentrations. In contrast, the transmission of camphor concordantly shows a similar low value for the PTR-MS (FAL).

Finally, it should be mentioned that the knowledge of the transmission is not necessary if a reliable calibration of the mass spectrometer for a certain compound is available. Even the rate constants and the reaction time are ultimately integrated in the calibration factor. But detailed considerations are required for compounds without a reliable calibration gas. Moreover, no investigations about the long-term stability of the transmission curve are available. But measurements by Ammann et al. [24] at least have shown that the aging of the secondary electron multiplier can mass-dependently affect the amplification of the signal and can consequently influence even the transmission function. Therefore, periodical evaluations of the transmission or calibrations are recommended.

### 3.3. Humidity dependence of the benzene sensitivity

Recently, Warneke et al. [18] have shown that the benzene sensitivity is strongly dependent on the humidity of the analyzed air. They attribute the humidity sensitivity to a discrepancy between the measured cluster ion distribution and the actual one in the drift tube. They relate it to a collision-induced dissociation (CID), which takes place between the drift tube and the quadrupole. As a consequence, more  $\text{H}_3\text{O}^+$  and less  $\text{H}_3\text{O}^+\text{H}_2\text{O}$  ions are measured because the water clusters dissociate back to the unhydrated form at the end of the drift tube. Benzene does not react with  $\text{H}_3\text{O}^+(\text{H}_2\text{O})_n$  clusters due to a too low proton affinity [18,33].

We performed measurements of the humidity dependence of benzene in the laboratory (room temperature 23 °C), using a gas standard with 0.75 ppm benzene (BOC Gase GmbH, Stuttgart, Germany), diluted with synthetic air by using two mass flow controllers, and a humidifier (LI-COR LI-610, Lincoln, NE, USA). The PTR-MS (PSI) was operated at  $p_{\text{drift}} = 2.08$  mbar,  $T_{\text{drift}} = 323$  K,  $U_{\text{drift}} = 570$  V, and  $E/N = 132.3$  Td conditions.  $E/N$  denotes the ratio of the electric field strength  $E$  and the buffer gas density  $N$ .

Fig. 5 shows the calibration curve for benzene ( $m/z$  79) at 5 different relative humidities. Considering the raw signal of  $m/z$  79 (see the inset in Fig. 5), no humidity dependence is observable. But, the primary ion signal is slightly changing with relative humidity, as shown in Fig. 6 including the raw signals of  $\text{H}_3^{18}\text{O}^+$  ( $m/z$  21) and of the water cluster  $\text{H}_3\text{O}^+\text{H}_2\text{O}$  ( $m/z$  37). The  $\text{H}_3\text{O}^+$  ion signal as well as the water cluster signal are rising with increasing humidity.

After standardizing the  $m/z$  79 signal to  $10^6$  cps  $\text{H}_3\text{O}^+$  primary ions, a humidity dependence (shown in the large plot of Fig. 5) is observed. This humidity dependence is similar but less distinct to that described by Warneke et al. [18]. The measurements presented in this work show a change in the sensitivity between dry and humid conditions of about

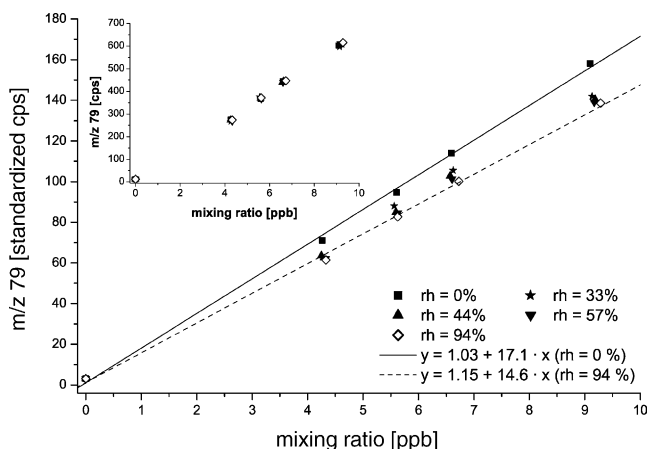


Fig. 5. Calibration curve of benzene. The small panel shows the raw signal of  $m/z$  79 (protonated benzene) vs. the benzene mixing ratio in the gas standard at five different relative humidity values. The large panel shows the standardized raw signal of  $m/z$  79 vs. the same  $x$ -axis. Standardization is described in the text.

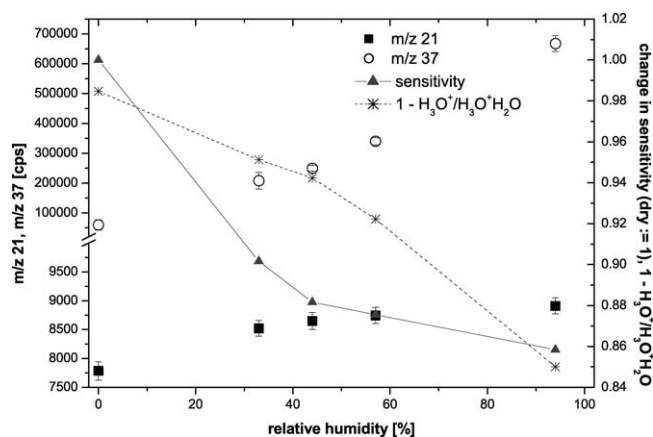


Fig. 6.  $\text{H}_3^{18}\text{O}^+$  ( $m/z$  21) and  $\text{H}_3\text{O}^+\text{H}_2\text{O}$  ( $m/z$  37) ions,  $1 - (\text{H}_3\text{O}^+ / \text{H}_3\text{O}^+\text{H}_2\text{O})$ , and the measured benzene sensitivity vs. the relative humidity.

16%, whereas Warneke et al. have detected a change of nearly 130%.

Warneke et al. [18] have developed a simple model that computes the cluster ion distribution in the drift tube. Using this model, it was possible to explain the dependence of the sensitivity on the humidity. For these studies, the authors have operated the PTR-MS at a drift tube pressure of 2.5 mbar. We performed similar tests with the PTR-MS (PSI) at a drift tube pressure of 2.08 mbar, which is equal to our standard operational conditions and is approximately the default value given by the manufacturer. Model calculations similar to those done by Warneke et al. do predict no cluster formation for a larger range of water concentrations. In contrast to that, we observed a dimer/monomer ratio of 1 to 15% between dry air and 100% humidity. These results are in accordance with another measurement to model comparison done by Hanson et al. [34] and de Gouw et al. [20] that also measured higher water cluster fractions than modeled at  $E/N$  above 110 Td. The model cannot accurately describe the cluster distribution in the drift tube since the measured distribution depends on the exact conditions in the drift tube and how the ions are extracted from the drift tube into the quadrupole mass spectrometer, the ion source water flow, and pumping characteristics. As seen from Fig. 6, there is no direct correlation between the measured sensitivity and the water cluster distribution. This can be explained by a less efficient CID at higher relative humidities or by a partly compensating production of water clusters in the jet that occurs due to the pressure drop between drift tube and quadrupole. Similar jets are a common tool for the production of dimers [35].

The biggest change in sensitivity (Fig. 5) appeared from absolutely dry to slightly humid conditions. This means that the effect in outdoor measurements should be small, because absolutely dry conditions do not occur in the troposphere. The slope decreases from 15.4 standardized cps per ppb at 33% relative humidity to 14.6 standardized cps per ppb at 94% relative humidity. Compared to the overall uncertainty of the measurement, this change of 5% can be neglected for many applications. However, it should be emphasized that the

effect has to be taken into account if the PTR-MS is calibrated under dry conditions and is operated under humid conditions.

### 3.4. Formaldehyde comparison

The proton affinity of formaldehyde (170.4 kcal/mol) is just slightly higher than that of water (165.2 kcal/mol) [23]. Therefore, the reaction of protonated HCHO with water becomes relevant and reduces the sensitivity. Hansel et al. [36] investigated the  $\text{H}_3\text{O}^+$  proton-transfer reaction to formaldehyde including the back reaction in a selected ion flow drift tube experiment (SIFT). They measured an energy dependence of the rate constants mainly for the backward reaction. For our conditions of the relative kinetic energy between the reactants ( $\text{KE}_{\text{cm}} = 0.17 \text{ eV}$ ), they found a rate constant of  $k_f \approx 1.5 \times 10^{-9} \text{ cm}^3 \text{ s}^{-1}$  for the forward and of  $k_b \approx 2.8 \times 10^{-11} \text{ cm}^3 \text{ s}^{-1}$  for the backward reaction.

We performed a laboratory intercomparison of HCHO with the PTR-MS (FAL) and a formaldehyde (Hantzsch) monitor. Different gaseous formaldehyde concentrations were produced with a permeation source and dilution with zero air. The permeation source was made out of a glass flask filled with *para*-formaldehyde and closed with a Tedlar film. The source was temperature stabilized at a temperature of  $50^\circ\text{C}$  in an oven integrated in the Hantzsch monitor. The Hantzsch monitor was calibrated by means of an aqueous formaldehyde solution ( $\approx 2 \mu\text{M}$ ).

Fig. 7 shows the results of the HCHO measurements. A linear relation between the data of the two instruments was obtained whereby the PTR-MS (FAL) observed only 21% of the HCHO measured by the Hantzsch monitor. However, the measurement of laboratory air right after this intercomparison resulted in a yield of 38% for the PTR-MS.

The intercomparison with the permeation source was carried out under dry conditions, whereas the laboratory air contained some humidity. But this cannot explain the different sensitivity. The backward reaction of protonated HCHO with

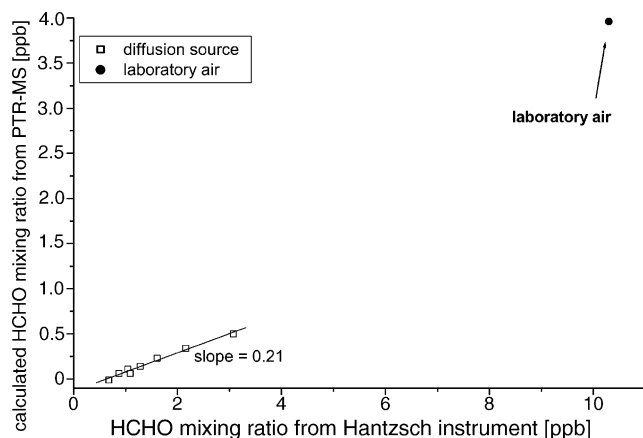


Fig. 7. Laboratory intercomparison between measurements of formaldehyde using PTR-MS and a Hantzsch monitor. The HCHO mixing ratio was calculated from the  $m/z$  31 signal according to Eq. (2) (reaction rate constant for formaldehyde protonation =  $2 \times 10^{-9} \text{ cm}^3 \text{ s}^{-1}$ ).

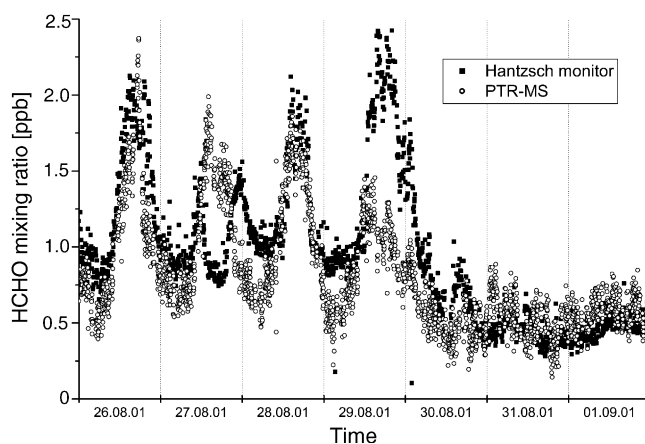


Fig. 8. Formaldehyde mixing ratios measured by PTR-MS and a Hantzsch monitor for a 7-day-period during the CHAPOP field campaign in southern Switzerland. The HCHO mixing ratio is calculated from the  $m/z$  31 signal according to Eq. (2) (reaction rate constant for formaldehyde protonation =  $2 \times 10^{-9} \text{ cm}^3 \text{ s}^{-1}$ ).

water should become more distinct under more humid conditions leading to a even lower sensitivity. For a humidity range between 20,000 and 80,000 ppm and  $10^4$  primary ions  $\text{cm}^{-3}$ , we predicted sensitivities of 37% to 10%. The higher recovery rate of the PTR-MS during the laboratory air measurement compared to the calibration mixture shows that an interference with some other compounds existing in the laboratory air cannot be excluded. A more detailed discussion follows at the end of the section.

A comparison of formaldehyde measurements in ambient air during the CHAPOP field campaign in southern Switzerland in summer 2001 is shown in Fig. 8. During days with low photochemical activity, low solar radiation (31 August–1 September), and low formaldehyde mixing ratios, the PTR-MS shows higher values than the Hantzsch monitor. During sunny days, the Hantzsch monitor (26–29 August) shows usually higher values, even during the night, when the mixing ratios are similar to the mixing ratios at low photochemical activity. But in contrast to the laboratory comparison, the PTR-MS always measures more than 50% of the Hantzsch monitor. It is interesting to note that on the afternoon of 27 August, the PTR-MS shows even significantly higher values than the fluorescent method. This happened in combination with an air mass exchange with advection of dry and clean air (so called foehn event) that caused a general decrease of nearly all pollutants and the relative humidity at the station. The Hantzsch monitor also shows this decrease whereas the PTR-MS produced a similar diurnal cycle as on the day before. A humidity dependence can be excluded, because the moisture remained small for the next 2 days after dropping on the 27th, and the Hantzsch instrument again shows higher values on the 28th and 29th. On the 29th, the highest HCHO mixing ratios of the whole period were measured by the Hantzsch method, whereas the PTR-MS concentrations were considerably lower than during the days before. This discrepancy cannot be related to meteorological conditions like relative

humidity, temperature and radiation. Several publications already show the feasibility of measuring formaldehyde by the fluorometric method used in this work [37,38]. Assuming that the formaldehyde data from the Hantzsch monitor are reliable, the field intercomparison finally showed unsatisfactory results for measuring HCHO by the PTR-MS.

Most probably other compounds or fragments of other compounds have contributed to the  $m/z$  31 signal. A possible candidate could be methyl hydroperoxide ( $\text{CH}_3\text{OOH}$ ), as one of its fragments contributes to the  $m/z$  31 signal (A. Hansel, personal communication). Staffelbach et al. [39] measured methyl hydroperoxide concentrations in southern Switzerland during summer 1994. They found mean mixing ratios ( $\pm$  standard deviation) for a 2-day-period of  $0.6 (\pm 0.23)$  ppb. Therefore, even if 100% of methyl hydroperoxide are fragmenting to  $m/z$  31 and assuming the calibrated sensitivity of 21%, it is hardly possible to explain the high  $m/z$  31 signal just by fragmentation of  $\text{CH}_3\text{OOH}$ . Nitric oxide (molecular weight 30 amu) does not play a role because of a too low proton affinity. But  $\text{NO}^+$  is produced at large quantities in the hollow cathode. The ionization energy of NO is so low that almost no charge transfer between NO and other compounds takes place after generating  $\text{NO}^+$  in the ion source. Due to an isotope ratio  $^{15}\text{N}/^{14}\text{N}$  of 0.37%,  $^{15}\text{NO}^+$  can contribute to  $m/z$  31 in a significant amount (about 1 ppb). This can be considered by subtracting 0.37% of the  $m/z$  30 signal. But no distinct reason for the different  $\text{HCHO}_{\text{Hantzsch}}/\text{HCHO}_{\text{PTR-MS}}$  ratios during the field campaign could be identified.

### 3.5. Instrument intercomparison

An intercomparison between the two PTR-MS systems was performed in the laboratory of the Paul Scherrer Institut in October 2002. Ambient air was sampled for one night just outside the laboratory in a rural environment. A calibration was performed before and after the intercomparison with a gas standard containing alkanes, alkenes, alkynes, dialkenes, and aromatics  $\leq \text{C}_9$  at concentrations of a few ppb (National Physical Laboratory, Teddington, UK). Mixing ratios were calculated based on these calibrations.

Fig. 9 shows the results for  $m/z$  107 (protonated  $\text{C}_2$ -benzenes) and  $m/z$  43 (protonated propene). The time series of  $m/z$  107 shows elevated mixing ratios in late afternoon and early morning as a consequence of increased traffic when people leave and arrive at the institute. Main sources of  $\text{C}_2$ -benzenes like xylenes and ethyl benzene are the evaporation of solvents and the evaporation and combustion of gasoline and to a lesser extent diesel [40]. Both mass spectrometers closely reproduce all the different features. A significant correlation ( $R^2 = 0.84$ ) and a slope of 1.14 with slightly higher values measured by the PTR-MS (FAL) is obtained (small panel in Fig. 9). Similar results with close correlations and slopes of  $1 \pm 0.2$  are also obtained e.g.,  $m/z$  57 (butene, butanol),  $m/z$  93 (toluene), and  $m/z$  121 (trimethylbenzene). Within the uncertainty of the measurements, the agreement between the two different instruments is satisfactory. Fig. 9b

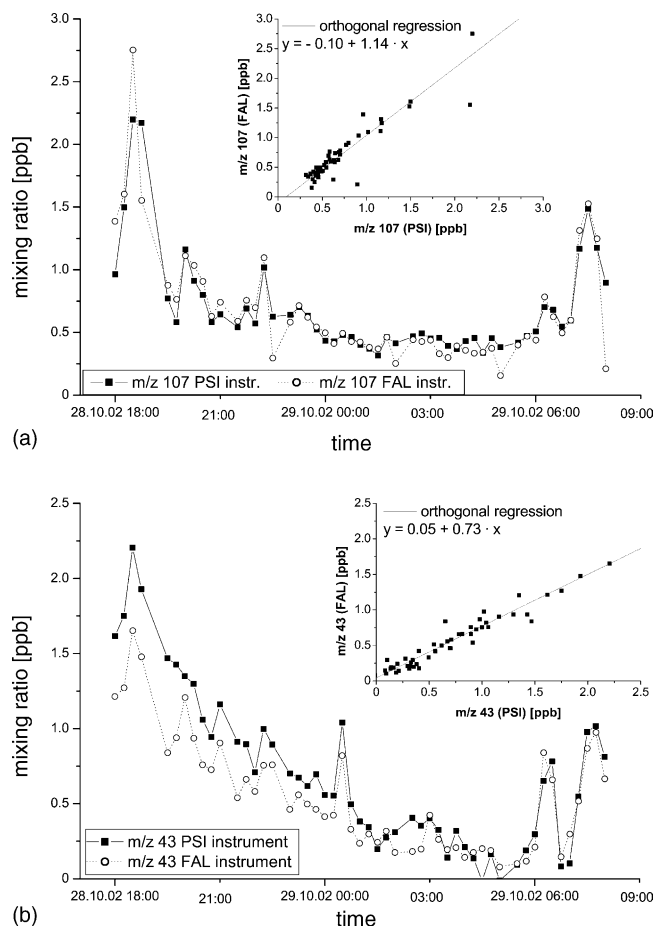


Fig. 9. Intercomparison of two PTR-MS systems. The data represent 15 min averages. One cycle took around 140 s, the dwell time for each mass during one cycle was 5 s. (a) Time series and scatter plot for  $m/z$  107 (protonated  $\text{C}_2$ -benzenes) and (b) time series and scatter plot for  $m/z$  43 (protonated propene).

shows the time series and the scatter plot for  $m/z$  43 which corresponds to protonated propene. It is emitted even in higher amounts by the traffic than the  $\text{C}_2$ -benzenes [41]. Propene shows also the highest mixing ratios in the late afternoon and an increase in the morning. There is a discrepancy between the PSI- and the FAL-instrument almost during the whole night, before they compare well in the morning. However, the scatter plot of the PTR-MS (FAL) data versus the PTR-MS (PSI) data shows a close correlation ( $R^2 = 0.93$ ) and a slope of just 0.73 for the whole dataset. Fragmentation of propene or other compounds on this mass might explain this discrepancy. The settings of the two instruments differed slightly (PSI-instrument:  $p_{\text{drift}} = 2.04$  mbar,  $U_{\text{drift}} = 580$  V,  $T_{\text{drift}} = 50$  °C,  $E/N = 137.1$  Td; FAL-instrument:  $p_{\text{drift}} = 2.04$  mbar,  $T_{\text{drift}} \approx T_{\text{air}} = 23$  °C,  $U_{\text{drift}} = 600$  V,  $E/N = 126.8$  Td), which could cause different fragmentation patterns. Warneke et al. [31] investigated the fragmentation patterns of 75 different VOCs with the PTR-MS, using a gas-chromatographic pre-separation method and reported major fragments appearing at  $m/z$  43 for 3-methyl-1-butene, 2-methyl-1-butene, 2-methyl-2-butene, trans-2-pentene, 1-pentene, and acetone. Other pos-



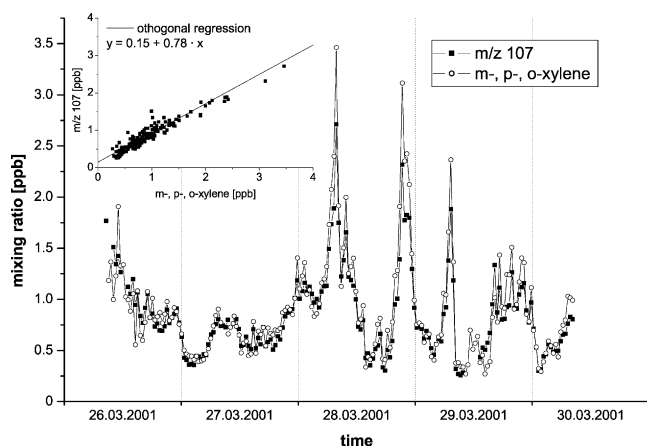


Fig. 10. Mixing ratios of the sum of xylenes (measured by the GC) and of  $m/z$  107 ( $C_2$ -benzenes; measured by PTR-MS) for a 5-day-period in Berne, Switzerland, in March 2001. Small panel: scatter plot of GC signal vs. PTR-MS signal ( $R^2 = 0.91$ ). Mixing ratios measured by PTR-MS were calculated according to Eq. (2).

sible species yielding a fragment of mass 43 are acetaldehyde, butanal, acetic acid and propanol. Tests with the PSI-instrument showed that propene fragments to 40% to mass 41, a mass 43 fragment yield of only 0.4% for acetaldehyde, and 5% for butanal.

### 3.6. Measurements of aromatics, PTR-MS comparison with GC

Fig. 10 shows the sum of xylenes measured by the GC and of  $m/z$  107 measured by the FAL-instrument during the campaign in Berne in March 2001. Mass 107 is attributed to  $C_2$ -benzenes (xylenes + ethyl benzene) and benzaldehyde. Benzaldehyde can be produced by the oxidative degradation of toluene [42]. Because of low temperatures and frequent rain during this period, we expect only a small contribution from this mechanism. Toluene and the  $C_2$ -benzenes as measured at this station are mostly emitted by the traffic. The emission factor of ethyl benzene from traffic is about one magnitude smaller than the emission factor of  $m$ -,  $p$ -xylene [41]. Therefore, the non-consideration of ethyl benzene by the GC does not change the results significantly. For the calculations of the concentrations (Eq. (2)), a weighted mean of the proton-transfer reaction rate constants ( $2.26 \times 10^{-9} \text{ cm}^3 \text{ s}^{-1}$ ) for the xylenes and ethyl benzene was used. The measurements with the two methods agree well regarding the diurnal pattern. The scatter plot of the PTR-MS signal versus the GC signal shows a high correlation ( $R^2 = 0.91$ ). On average, 78% of the concentration quantified by the GC is found by the PTR-MS as denoted by the slope of the regression line. The correlation (not shown here) between  $m/z$  93 (protonated toluene; measured by PTR-MS) and toluene (measured by GC) shows a slope of 0.86 ( $R^2 = 0.89$ ). Losses in the instrument itself can probably cause the slightly lower concentrations measured by PTR-MS because the ambient air still passed a mass flow controller before the drift tube at the time of these measure-

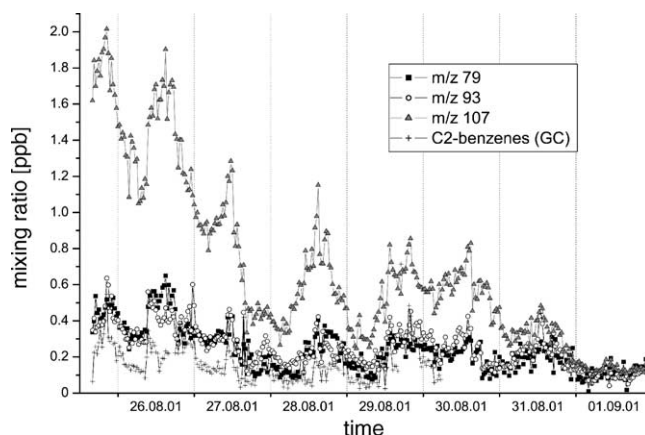


Fig. 11. Mixing ratios of benzene ( $m/z$  79), toluene ( $m/z$  93),  $C_2$ -benzenes + benzaldehyde ( $m/z$  107; measured by PTR-MS), and the  $C_2$ -benzenes (xylenes + ethyl benzene; measured by GC) for a 7-day-period during the CHAPOP field campaign in southern Switzerland. Mixing ratios measured by PTR-MS were calculated according to Eq. (2).

ments. As mentioned above, the theoretically calculated reaction rate constants might show an uncertainty of  $\pm 20\%$  [12,14]. Within these and the uncertainties of the GC measurements (uncertainty  $< \pm 25\%$  [43]), no systematic discrepancy seems to exist and the agreement between the two techniques can be regarded as satisfactory. The reliability of the measurements is also corroborated considering the toluene ( $m/z$  93) to benzene ( $m/z$  79) ratio of 2.2, which is a typical value for fresh traffic emissions [41].

During the CHAPOP campaign, clear sky and temperatures up to  $27^\circ\text{C}$  were characteristic for the intensive operation period from 26 to 29 August. Afterwards, the meteorological situation changed to lower temperatures and overcast conditions. Fig. 11 shows some aromatic compounds measured by PTR-MS and GC. There is a big discrepancy between the  $m/z$  107 signal and the  $C_2$ -benzene mixing ratios of the GC. Moreover, the  $m/z$  107 signal is significantly higher than the  $m/z$  93 and  $m/z$  79 signals. This is most pronounced during the period of high photochemical activity and becomes less distinct at the end of the presented period. Benzaldehyde, which is most of all produced by the toluene degradation contributes to the  $m/z$  107 signal of the mass spectrometer. Estimates taking into account typical emission factors, OH reactivities of the aromatics and a benzaldehyde yield of 6% out of the toluene oxidation [44] cannot reproduce the measured concentrations. Because of a good correlation of the signal attributed to benzaldehyde with the indoor temperature, we initially presumed a contamination due to a possible leakage and some outgassing in the container. But the sudden decline of  $m/z$  107 at around noon of the 27th (due to the foehn event mentioned in Section 3.4) and the correlation of this signal with other VOCs like benzene do not support this hypothesis. Unexplained contributions to  $m/z$  107 contradict the data of de Gouw et al. [20] and Warneke et al. [31], who performed GC-PTR-MS measurements at urban and remote stations. Both publications reported no interfering signals at

$m/z$  107. As our sampling site is surrounded by grassland and trees, the air is burdened by VOCs of biogenic and anthropogenic origin. There are no VOCs of biogenic origin with  $m/z$  107 reported in the literature. It is also difficult to imagine such considerable amounts of other anthropogenically emitted compounds with that mass in the atmospheric boundary layer. However, a contribution of a directly emitted or photochemically oxidized biogenic VOC cannot be excluded. There seems to be a correlation between  $m/z$  107 and the photochemical activity of the air mass as presented in the following. A possible correlation is also corroborated by reaction chamber studies of the photooxidation of  $\alpha$ -pinene at the Paul Scherrer Institute (unpublished results). They showed a clearly visible signal on  $m/z$  107, 1–4 h after the start of the pinene degradation.

Fig. 12 shows a scatter plot of the  $C_2$ -benzenes mixing ratio (GC) versus the  $m/z$  93 (attributed to toluene) mixing ratio (panel a) and a scatter plot of  $m/z$  107 ( $C_2$ -benzenes + benzaldehyde) versus  $m/z$  93 (panel b). In Fig. 12b, the data are separated in four time periods with

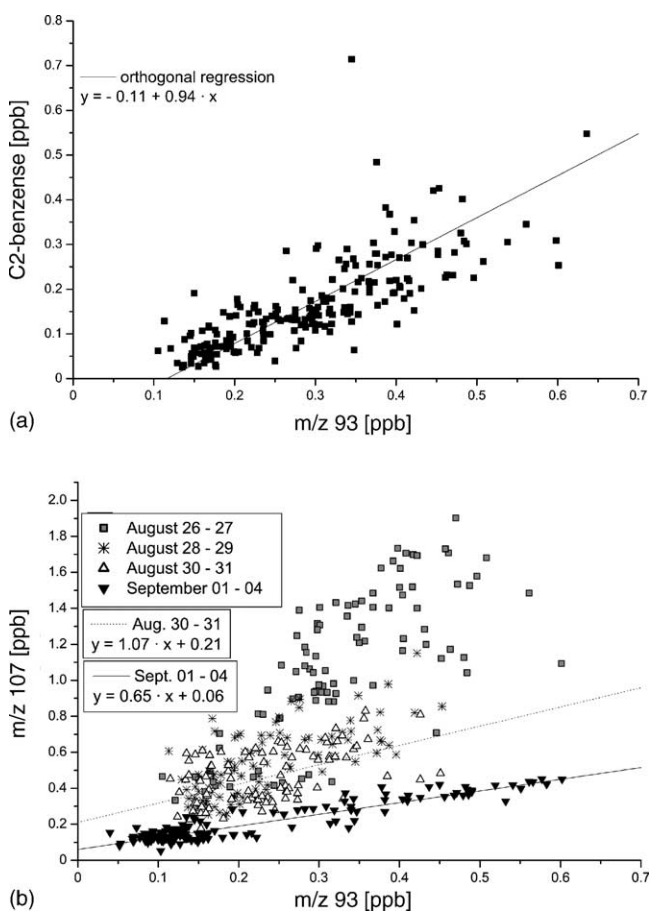


Fig. 12. (a) Scatter plot of  $C_2$ -benzenes (measured by GC) vs.  $m/z$  93 (attributed to toluene; measured by PTR-MS). (b) Scatter plot of  $m/z$  107 (attributed to  $C_2$ -benzenes + benzaldehyde) vs.  $m/z$  93 (both measured by PTR-MS). Mixing ratios measured by PTR-MS were calculated according to Eq. (2). Measurements were performed during the CHAPOP field campaign in southern Switzerland.

different meteorological conditions. It is obvious that the linear regression slopes decreased within the whole period presented here. For 26–27 August, the slope reaches nearly 3 (not shown in Fig. 12b). Later the slope ranges around 1 (30–31 August) in agreement with the data in panel a, and becomes even smaller at the end of the measurements. The degree of photochemical processing definitely influences the amount of benzaldehyde in the atmosphere and influences, therefore, the  $m/z$  107 signal of the mass spectrometer, too. The  $m/z$  107 to 93 data recorded from 1 to 4 September show the best correlation. This can be ascribed to identical sources and no significant (photochemical) conversion of the contributing species to  $m/z$  107 and 93. The fact that this slope is lower than the slope of panel a might indicate a slight under prediction of the PTR-MS measurements.

#### 4. Conclusions

Extensive laboratory and field measurements have revealed important characteristics concerning the performance of the two different versions of the PTR-MS instrument. The features investigated include the background signal stability, the transmission efficiency, the humidity dependence, a comparison with a formaldehyde monitor, an instrument intercomparison, and a comparison with a gas chromatograph.

The newer instrument (PSI) with a temperature stabilization of the inlet system and the drift tube as well as Teflon gaskets instead of Viton performed considerably better with respect to signal stability. The background variability as well as the general background level was diminished significantly in the newer version. The maximum daily variation has diminished from 0.27, 0.51, and 0.25 to 0.04, 0.07, and 0.03 ppb for  $m/z$  79, 107, and 121, respectively. The average blank values decreased from 0.36, 0.25, and 0.13 to 0.04, 0.05, and 0.05 ppb for  $m/z$  79, 107, and 121, respectively. But even with Teflon seals, frequent background measurements are still recommended to be able to consider potential memory effects or influences of other environmental parameters. During our field campaign background measurements were performed for 30 min every 3 h.

A reliable knowledge of the mass discrimination of the PTR-MS is essential to calculate the mixing ratios of VOCs following the PTR-MS theory. The method proposed in this work with injecting small volumes of liquid compounds into pillow bags seems to be a feasible way to determine the function. The measurements are quickly reaching stable conditions, but are not perfectly reproducible so that the data is characterized by a large scatter. Even if this variability is considered, the curve determined here does not coincide with the curve given by the manufacturer. The transmission determination by the manufacturer might have been performed at different instrumental settings than those used by us. As a consequence, a determi-

nation by the user is highly recommended. A wrong transmission function might be responsible for errors of around 25%.

In contrast to the humidity sensitivity for benzene measurements reported by Warneke et al. [18] at a drift tube pressure of 2.5 mbar, we found a much less distinct effect. The effect was largest when changing from absolutely dry to slightly humid conditions. Therefore, the effect has to be taken into account in the case of dry calibration conditions. A comparison of the measured and the modeled primary ion cluster distribution showed the inability of the model to reproduce the measurements. An overproportional increase of the dimer/monomer ratio with humidity may even point to a cluster producing process like a dimer generation in the jet entering the quadrupole is supposed.

As already reported in the literature [36,45], the measurement of formaldehyde with the PTR-MS is problematic due to the low proton affinity of this molecule. The comparison of the PTR-MS with a formaldehyde monitor showed for a dry gaseous HCHO mixture a significant correlation and a sensitivity of 21%. A comparison with laboratory air and during a field campaign showed a significantly larger sensitivity of  $m/z$  31 of the PTR-MS compared with the formaldehyde monitor. This can probably be attributed to an interference due to isobaric compounds or fragments.

The intercomparison between two different PTR-MSs presented satisfactory results for several different masses but pointed again to one of the general problems of PTR-MS measurements. Even if a reliable calibration source is available, a contribution of isobaric molecules can never be excluded because of the mass and not species-specific sensitivity of the PTR-MS. This comparison has shown furthermore, that the particular settings of the instrument might change the response of the system to changing environmental conditions. Therefore, a detailed characterization of the instrument for these particular settings is strongly recommended.

Atmospheric measurements in cases of low photo-oxidation conditions showed a good agreement between gas chromatography and proton-transfer reaction mass spectrometry for aromatics. Under conditions of high insolation, biogenic as well as anthropogenic VOC sources and photochemically processed air, a substantial discrepancy between the  $m/z$  107 concentration of the PTR-MS and the  $C_2$ -benzene concentration of the GC appeared. Known yields of benzaldehyde from the toluene oxidation could not reproduce the differences. Therefore, an unknown compound can significantly contribute to  $m/z$  107 under certain conditions.

As seen in this work, unknown contributors to a certain mass and the fragmentation which is sensitive to the instrument specific settings can complicate the interpretation of the mass spectra considerably. Parallel measurements with another technique (e.g., gas chromatography), therefore, ideally complete PTR-MS studies even if they only provide data at lower time resolutions.

## Acknowledgements

We thank Hanspeter Burn and the Cantonal Office for Industry, Trade and Employment, Berne to provide some space for the measurements in Berne. We thank Stephan Henne and Carlos Ordóñez for their support during the field campaigns, Jaša Čalagović for performing laboratory tests, and Stefan Reimann for checking our gas standards. We also thank Carsten Warneke for helpful discussions. This work was supported by the Swiss National Science Foundation under Grant No. 21-61573.00. The FORMAT Project was funded by the Research Directorate of the European Commission under Grant No. EVK2-CT-2001-00120.

## References

- [1] W. Lindinger, A. Hansel, A. Jordan, *Int. J. Mass Spectrom. Ion Process* 173 (1998) 191.
- [2] P.J. Crutzen, J. Williams, U. Pöschl, P. Hoor, H. Fischer, C. Warneke, R. Holzinger, A. Hansel, W. Lindinger, B. Scheeren, J. Lelieveld, *Atmos. Environ.* 34 (2000) 1161.
- [3] R. Holzinger, L. Sandoval-Soto, S. Rottenberger, P.J. Crutzen, J. Kesselmeier, *J. Geophys. Res.* 105 (20) (2000) 573.
- [4] T. Karl, P.J. Crutzen, M. Mandl, M. Staudinger, A.B. Guenther, A. Jordan, R. Fall, W. Lindinger, *Atmos. Environ.* 35 (2001) 5287.
- [5] A. Boschetti, F. Biasioli, M. van Opbergen, C. Warneke, A. Jordan, R. Holzinger, P. Prazeller, T. Karl, A. Hansel, W. Lindinger, S. Iannotta, *Postharvest Biol. Technol.* 17 (1999) 143.
- [6] C. Yeretizian, A. Jordan, W. Lindinger, *Int. J. Mass Spectrom.* 223–224 (2003) 115.
- [7] D. Mayr, R. Margesin, F. Schinner, T.D. Märk, *Int. J. Mass Spectrom.* 223–224 (2003) 229.
- [8] W. Lindinger, J. Taucher, A. Jordan, A. Hansel, W. Vogel, *Alcohol Clin. Exp. Res.* 21 (1997) 939.
- [9] J. Taucher, A. Hansel, A. Jordan, R. Fall, J.H. Futrell, W. Lindinger, *Rapid Commun. Mass Spectrom.* 11 (1997) 1230.
- [10] P. Prazeller, T. Karl, A. Jordan, R. Holzinger, A. Hansel, W. Lindinger, *Int. J. Mass Spectrom.* 178 (1998) 1.
- [11] T. Karl, P. Prazeller, D. Mayr, A. Jordan, J. Rieder, R. Fall, W. Lindinger, *J. Appl. Physiol.* 91 (2001) 762.
- [12] A. Hansel, A. Jordan, R. Holzinger, P. Prazeller, W. Vogel, W. Lindinger, *Int. J. Mass Spectrom. Ion Process* 149–150 (1995) 609.
- [13] W. Lindinger, A. Hansel, A. Jordan, *Chem. Soc. Rev.* 27 (1998) 347.
- [14] A. Hansel, A. Jordan, C. Warneke, R. Holzinger, A. Wisthaler, W. Lindinger, *Plasma Sources Sci. Technol.* 8 (1999) 332.
- [15] G. Gioumousis, D.P. Stevenson, *J. Chem. Phys.* 29 (1958) 294.
- [16] T. Su, M.T. Bowers, *Int. J. Mass Spectrom. Ion Phys.* 12 (1973) 347.
- [17] T. Su, W.J. Chesnavich, *J. Chem. Phys.* 76 (1982) 5183.
- [18] C. Warneke, C. van der Veen, S. Luxembourg, J.A. de Gouw, A. Kok, *Int. J. Mass Spectrom.* 207 (2001) 167.
- [19] S. Hayward, C.N. Hewitt, J.H. Sartin, S.M. Owen, *Environ. Sci. Technol.* 36 (2002) 1554.
- [20] J.A. de Gouw, C. Warneke, T. Karl, G. Eerdekens, C. van der Veen, R. Fall, *Int. J. Mass Spectrom.* 223–224 (2003) 365.
- [21] W. Lindinger, A. Hansel, *Plasma Sources Sci. Technol.* 6 (1997) 111.
- [22] A. Hansel, A. Jordan, C. Warneke, R. Holzinger, W. Lindinger, *Rapid Commun. Mass Spectrom.* 12 (1998) 871.
- [23] NIST Chemistry Webbook, <http://webbook.nist.gov/chemistry/paser.html>, 2004.

- [24] C. Ammann, C. Spirig, A. Neftel, M. Steinbacher, M. Komenda, A. Schaub, *Int. J. Mass Spectrom.* 239 (2004) 87.
- [25] A. Tani, S. Hayward, C.N. Hewitt, *Int. J. Mass Spectrom.* 223–224 (2003) 561.
- [26] J. Barker, *Mass Spectrometry*, second ed., Wiley, Chichester, 1999.
- [27] W. Lindinger, in: J.H. Futrell (Ed.), *Gaseous Ion Chemistry and Mass Spectrometry*, Wiley, New York, 1986 (Chapter 11).
- [28] W.J. Chesnavich, T. Su, M.T. Bowers, *J. Chem. Phys.* 72 (1980) 2641.
- [29] S. Konrad, A. Volz-Thomas, *J. Chromatogr. A* 878 (2000) 215.
- [30] T.J. Kelly, C.R. Fortune, *Int. J. Environ. Anal. Chem.* 54 (1994) 249.
- [31] C. Warneke, J.A. de Gouw, W.C. Kuster, P.D. Goldan, R. Fall, *Environ. Sci. Technol.* 37 (2003) 2494.
- [32] P.H. Dawson, *Quadrupole Mass Spectrometry and its Applications*, Elsevier Scientific Publishing Company, Amsterdam, 1976.
- [33] D. Smith, A.M. Diskin, Y. Ji, P. Spanel, *Int. J. Mass Spectrom.* 209 (2001) 81.
- [34] D.R. Hanson, J. Greenberg, B.E. Henry, E. Kosciuch, *Int. J. Mass Spectrom.* 223–224 (2003) 507.
- [35] L.H. Coudert, F.J. Lovas, R.D. Suenram, J.T. Hougen, *J. Chem. Phys.* 87 (1987) 6290.
- [36] A. Hansel, W. Singer, A. Wisthaler, M. Schwarzmann, W. Lindinger, *Int. J. Mass Spectrom. Ion Process* 167–168 (1997) 697.
- [37] J. Slemr, W. Junkermann, A. Volz-Thomas, *Atmos. Environ.* 30 (1996) 3667.
- [38] L.M. Cárdenas, D.J. Brassington, B.J. Allan, H. Coe, B. Alicke, U. Platt, K.M. Wilson, J.M.C. Plane, S.A. Penkett, *J. Atmos. Chem.* 37 (2000) 53.
- [39] T. Staffelbach, A. Neftel, A. Blatter, A. Gut, M. Fahrni, J. Staehelin, A.S.H. Prévôt, A.M. Hering, M. Lehning, B. Neining, M. Bäumle, G.L. Kok, J. Dommen, M. Hutterli, M. Anklin, *J. Geophys. Res.* 102 (1997) 23345.
- [40] N.V. Heeb, A.-M. Forss, C. Bach, S. Reimann, A. Herzog, H.W. Jäckle, *Atmos. Environ.* 34 (2000) 3103.
- [41] J. Staehelin, C. Keller, W. Stahel, K. Schläpfer, S. Wunderli, *Atmos. Environ.* 32 (1998) 999.
- [42] J.H. Seinfeld, S.N. Pandis, *Atmospheric Chemistry and Physics: From Air Pollution to Climate Change*, Wiley, New York, 1998.
- [43] A.S.H. Prévôt, J. Dommen, M. Bäumle, *Atmos. Environ.* 34 (2000) 4719.
- [44] B. Klotz, S. Sørensen, I. Barnes, K.H. Becker, T. Eitzkorn, R. Volkamer, U. Platt, K. Wirtz, M. Martín-Reviejo, *J. Phys. Chem. A* 102 (1998) 10289.
- [45] R. Holzinger, C. Warneke, A. Hansel, A. Jordan, W. Lindinger, D.H. Scharffe, G. Schade, P.J. Crutzen, *Geophys. Res. Lett.* 26 (1999) 1161.